JACS
JOURNAL OF THE AMERICAN CHEMICAL SOCIETY

Subscriber access provided by ISTANBUL TEKNIK UNIV

Article

Two-Dimensional Combinatorial Screening Identifies Specific Aminoglycoside#RNA Internal Loop Partners

Matthew D. Disney, Lucas P. Labuda, Dustin J. Paul, Shane G. Poplawski, Alexei Pushechnikov, Tuan Tran, Sai P. Velagapudi, Meilan Wu, and Jessica L. Childs-Disney

J. Am. Chem. Soc., **2008**, 130 (33), 11185-11194 • DOI: 10.1021/ja803234t • Publication Date (Web): 25 July 2008

Downloaded from http://pubs.acs.org on February 8, 2009

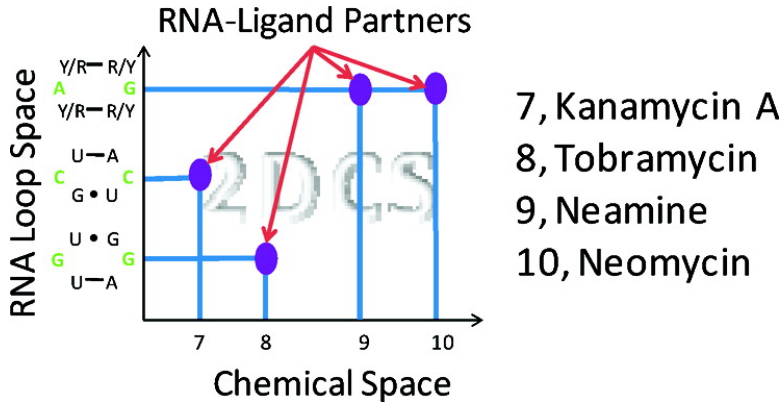

More About This Article

Additional resources and features associated with this article are available within the HTML version:

- Supporting Information
- Links to the 2 articles that cite this article, as of the time of this article download
- Access to high resolution figures
- Links to articles and content related to this article
- Copyright permission to reproduce figures and/or text from this article

View the Full Text HTML

ACS Publications
High quality. High impact.

Journal of the American Chemical Society is published by the American Chemical Society. 1155 Sixteenth Street N.W., Washington, DC 20036

J|A|C|S
ARTICLES

Published on Web 07/25/2008

Two-Dimensional Combinatorial Screening Identifies Specific Aminoglycoside−RNA Internal Loop Partners

Matthew D. Disney,*,† Lucas P. Labuda,† Dustin J. Paul,† Shane G. Poplawski,‡ Alexei Pushechnikov,† Tuan Tran,† Sai P. Velagapudi,† Meilan Wu,† and Jessica L. Childs-Disney‡

Department of Chemistry, University at Buffalo, The State University of New York, and the New York State Center of Excellence in Bioinformatics and Life Sciences, 657 Natural Sciences Complex, Buffalo, New York 14260, and Department of Chemistry & Biochemistry, Canisius College, 2001 Main Street, Buffalo, New York 14208

Received May 1, 2008; E-mail: mddisney@buffalo.edu

Abstract: Herein is described the identification of RNA internal loops that bind to derivatives of neomycin B, neamine, tobramycin, and kanamycin A. RNA loop−ligand partners were identified by a two-dimensional combinatorial screening (2DCS) platform that probes RNA and chemical spaces simultaneously. In 2DCS, an aminoglycoside library immobilized onto an agarose microarray was probed for binding to a 3 × 3 nucleotide RNA internal loop library (81 920 interactions probed in duplicate in a single experiment). RNAs that bound aminoglycosides were harvested from the array via gel excision. RNA internal loop preferences for three aminoglycosides were identified from statistical analysis of selected structures. This provides consensus RNA internal loops that bind these structures and include: loops with potential GA pairs for the neomycin derivative, loops with potential GG pairs for the tobramycin derivative, and pyrimidine-rich loops for the kanamycin A derivative. Results with the neamine derivative show that it binds a variety of loops, including loops that contain potential GA pairs that also recognize the neomycin B derivative. All studied selected internal loops are specific for the aminoglycoside that they were selected to bind. Specificity was quantified for 16 selected internal loops by studying their binding to each of the arrayed aminoglycosides. Specificities ranged from 2- to 80-fold with an average specificity of 20-fold. These studies show that 2DCS is a unique platform to probe RNA and chemical space simultaneously to identify specific RNA motif−ligand interactions.

Introduction

RNA is an important target for therapeutic intervention due to its essential biological functions.[1–8] These functions are often predicated on both the RNA sequence and structure. The most commonly exploited RNA drug target for small-molecule intervention is bacterial rRNA. [9,10] Other less explored RNA drug targets are pre-microRNAs that are processed into microRNAs,[1,11] which play important roles in regulating gene expression[12,13] and diseases such as cancer.[14,15] Small molecules can also target mRNA by binding to riboswitches in untranslated regions[5,6,16–18] or in the coding regions themselves. Part of the reason for the underexploitation of RNA drug targets is the limited information available on the RNA secondary structure motifs that bind small molecules and the features in small molecules that are important for binding RNA structures. If such information were known, then it would facilitate the development of improved methods for the design of probes or drugs targeting RNA.

There are two main methods currently used to identify RNA−ligand interactions: selective evolution of ligands by exponential enrichment (SELEX) and high-throughput screening of small molecules. SELEX finds an RNA that binds a ligand

† University at Buffalo, The State University of New York, and the New York State Center of Excellence in Bioinformatics and Life Sciences.
‡ Canisius College.

(1) Lau, N. C.; Lim, L. P.; Weinstein, E. G.; Bartel, D. P. *Science* **2001**, *294*, 858–62.
(2) Zaug, A. J.; Cech, T. R. *Science* **1986**, *231*, 470–5.
(3) Guerrier-Takada, C.; Gardiner, K.; Marsh, T.; Pace, N.; Altman, S. *Cell* **1983**, *35*, 849–57.
(4) Vonahsen, U.; Noller, H. F. *Science* **1993**, *260*, 1500–3.
(5) Winkler, W. C.; Cohen-Chalamish, S.; Breaker, R. R. *Proc. Natl. Acad. Sci. U.S.A.* **2002**, *99*, 15908–13.
(6) Winkler, W.; Nahvi, A.; Breaker, R. R. *Nature* **2002**, *419*, 952–6.
(7) Gallego, J.; Varani, G. *Acc. Chem. Res.* **2001**, *34*, 836–43.
(8) Disney, M. D.; Childs, J. L.; Turner, D. H. *Biopolymers* **2004**, *73*, 151–61.
(9) Tenson, T.; Mankin, A. *Mol. Microbiol.* **2006**, *59*, 1664–77.
(10) Poehlsgaard, J.; Douthwaite, S. *Nat. Rev. Microbiol.* **2005**, *3*, 870–81.
(11) Lagos-Quintana, M.; Rauhut, R.; Lendeckel, W.; Tuschl, T. *Science* **2001**, *294*, 853–8.
(12) He, Y. D.; Friedman, A.; Perrimon, N.; Medina-Martinez, O.; Jamrich, M.; Zhao, Y.; Srivastava, D.; Miller, L. D.; Liu, E. T. *Cancer Biomark.* **2006**, *2*, 103–33.
(13) Zhao, Y.; Srivastava, D. *Trends Biochem. Sci.* **2007**, *32*, 189–97.
(14) Calin, G. A.; Croce, C. M. *Oncogene* **2006**, *25*, 6202–10.
(15) Yeung, M. L.; Bennasser, Y.; Jeang, K. T. *Curr. Med. Chem.* **2007**, *14*, 191–7.
(16) Nahvi, A.; Sudarsan, N.; Ebert, M. S.; Zou, X.; Brown, K. L.; Breaker, R. R. *Chem. Biol.* **2002**, *9*, 1043–9.
(17) Blount, K. F.; Breaker, R. R. *Nat. Biotechnol.* **2006**, *24*, 1558–64.
(18) Blount, K. F.; Wang, J. X.; Lim, J.; Sudarsan, N.; Breaker, R. R. *Nat. Chem. Biol.* **2007**, *3*, 44–9.

 © 2008 American Chemical Society

by multiple rounds of selection.[19] These RNA−ligand complexes can be used as sensors[20] or as biochemical tools.[21] The aptamer−ligand complex that is the output of SELEX, however, is difficult to apply to RNA targeting endeavors because the selected RNAs are large (derived from a ≥20-nucleotide random region)[19,22] and unlikely to be found in a biologically relevant RNA. Despite this impediment, there have been cases where parts of an RNA aptamer identified via SELEX have been found in a biological RNA.[23,24] In high-throughput screening of small molecules, the more common approach in RNA drug discovery, a library of chemical ligands is probed for binding a validated RNA drug target such as the bacterial rRNA aminoacyl-tRNA site (A-site),[25–30] HIV trans-activating responsive element (TAR) and Rev responsive element (RRE) RNAs,[31,32] or the hepatitis C internal ribosomal entry site.[33,34] When applied toward "druglike ligands", however, high-throughput screening has been hampered by low hit rates, much lower rates than are typically found by screening protein targets. Part of the reason for this is little is known about what types of RNA structures like to bind organic ligands and what types of organic ligands like to bind RNA structures.

By merging chemical (high-throughput screening of drugs) and RNA (selection) screening, we envision that features in both the RNA and ligand that facilitate molecular recognition can be identified.[35,36] This would be especially useful if the RNAs identified that bound ligands were small RNA motifs (hairpins, loops, or bulges) that are typically found in RNA targets. These results could help to establish a database that could serve as a rational design tool for the modular construction of RNA-targeting ligands. We previously reported a chemical microarray[35–45] platform to screen RNA libraries for binding small molecules.[35] In that report, a selection was completed by use of an RNA internal loop library and 6′-N-derivatized kanamycin A. It was determined that the kanamycin derivative preferred loops with potential AC pairs. The platform was also used to demonstrate that an array with four related aminoglycosides could be probed simultaneously for binding to an RNA library. The RNAs that bound to each aminoglycoside, however, were not sequenced nor were their binding affinities studied. Herein, we describe the results from screening chemical and RNA spaces simultaneously (named two-dimensional combinatorial screening, 2DCS) to find the small RNA internal loops that bind to derivatives of four aminoglycosides (kanamycin A, tobramycin, neamine, and neomycin B). Results show that the RNA motif−ligand partners identified by 2DCS are specific for the aminoglycosides for which they were selected. Sequencing and structure modeling of the selected internal loops show that neomycin prefers loops with potential GA pairs, tobramycin prefers RNA internal loops with potential GG pairs, and kanamycin A prefers internal loops with potential pyrimidine−pyrimidine pairs. Neamine binds to a variety of internal loops, including internal loops with potential GA pairs.

Materials and Methods

Synthesis. All azido-aminoglycosides were synthesized from the corresponding free base forms of the parent aminoglycosides according to previously published procedures.[35–37] The azido-aminoglycosides were fluorescently labeled with 5-fluorescein isothiocyanate (5-FITC, Toronto Research Chemicals) by a two-step procedure in which the Boc-protected azido-aminoglycosides were reacted with propargylamine to install a free amine that was then conjugated to 5-FITC.[46]

Construction of Alkyne-Displaying Microarrays. Microarrays were constructed as described.[35,36] Briefly, ~2 mL of a 1% agarose solution was applied to a Silane-Prep slide (Sigma−Aldrich Co., St. Louis, MO), and the agarose was allowed to dry to a thin film at room temperature. The agarose was oxidized by submerging the slides in 20 mM $NaIO_4$ for 30 min.[47] The oxidized agarose slides were then washed in water (3 × 30 min) with frequent water changes. Residual $NaIO_4$ was removed by incubating the slides in 10% aqueous ethylene glycol for 1.5 h at room temperature, which was followed by washing with water as described above. The slides were then incubated with 20 mM propargylamine in 0.1 M $NaHCO_3$ overnight and reduced with $NaCNBH_3$ the following morning (100 mg in 40 mL of 1× phosphate-buffered saline + 10 mL of ethanol; 3 min at room temperature). Slides were washed with water and dried before use.

Construction of Azido-aminoglycoside Microarrays. Azido-aminoglycosides were spotted onto alkyne-functionalized slides in 10 mM Tris-HCl (pH 8.5), 100 μM tris(benzyltriazolylmethyl)amine (TBTA)[48] (dissolved in 4:1 butanol/dimethyl sulfoxide, DMSO), 1 mM $CuSO_4$, 1 mM ascorbic acid, and 10% glycerol. The slides were placed into a humidity chamber for 2 h and then washed with water. The slides were dried at room temperature.

(19) Osborne, S. E.; Ellington, A. D. *Chem. Rev.* **1997**, *97*, 349–70.
(20) Ellington, A. D.; Szostak, J. W. *Nature* **1990**, *346*, 818–22.
(21) Werstuck, G.; Green, M. R. *Science* **1998**, *282*, 296–8.
(22) Joyce, G. F. *Curr. Opin. Struct. Biol.* **1994**, *4*, 331–6.
(23) Tao, J.; Frankel, A. D. *Biochemistry* **1996**, *35*, 2229–38.
(24) Carlson, C. B.; Vuyisich, M.; Gooch, B. D.; Beal, P. A. *Chem. Biol.* **2003**, *10*, 663–72.
(25) Wong, C. H.; Hendrix, M.; Manning, D. D.; Rosenbohm, C.; Greenberg, W. A. *J. Am. Chem. Soc.* **1998**, *120*, 8319–27.
(26) Disney, M. D.; Seeberger, P. H. *Chemistry* **2004**, *10*, 3308–14.
(27) Swayze, E. E.; Jefferson, E. A.; Sannes-Lowery, K. A.; Blyn, L. B.; Risen, L. M.; Arakawa, S.; Osgood, S. A.; Hofstadler, S. A.; Griffey, R. H. *J. Med. Chem.* **2002**, *45*, 3816–9.
(28) Jefferson, E. A.; Arakawa, S.; Blyn, L. B.; Miyaji, A.; Osgood, S. A.; Ranken, R.; Risen, L. M.; Swayze, E. E. *J. Med. Chem.* **2002**, *45*, 3430–9.
(29) Yu, L.; Oost, T. K.; Schkeryantz, J. M.; Yang, J.; Janowick, D.; Fesik, S. W. *J. Am. Chem. Soc.* **2003**, *125*, 4444–50.
(30) Disney, M. D.; Magnet, S.; Blanchard, J. S.; Seeberger, P. H. *Angew. Chem., Int. Ed.* **2004**, *43*, 1591–4.
(31) Mei, H. Y.; Mack, D. P.; Galan, A. A.; Halim, N. S.; Heldsinger, A.; Loo, J. A.; Moreland, D. W.; Sannes-Lowery, K. A.; Sharmeen, L.; Truong, H. N.; Czarnik, A. W. *Bioorg. Med. Chem.* **1997**, *5*, 1173–84.
(32) Peled-Zehavi, H.; Horiya, S.; Das, C.; Harada, K.; Frankel, A. D. *RNA* **2003**, *9*, 252–61.
(33) Seth, P. P.; Miyaji, A.; Jefferson, E. A.; Sannes-Lowery, K. A.; Osgood, S. A.; Propp, S. S.; Ranken, R.; Massire, C.; Sampath, R.; Ecker, D. J.; Swayze, E. E.; Griffey, R. H. *J. Med. Chem.* **2005**, *48*, 7099–102.
(34) Jefferson, E. A.; Seth, P. P.; Robinson, D. E.; Winter, D. K.; Miyaji, A.; Osgood, S. A.; Swayze, E. E.; Risen, L. M. *Bioorg. Med. Chem. Lett.* **2004**, *14*, 5139–43.
(35) Childs-Disney, J. L.; Wu, M.; Pushechnikov, A.; Aminova, O.; Disney, M. D. *ACS Chem. Biol.* **2007**, *2*, 745–54.
(36) Disney, M. D.; Childs-Disney, J. L. *ChemBioChem* **2007**, *8*, 649–56.
(37) Disney, M. D.; Barrett, O. J. *Biochemistry* **2007**, *46*, 11223–30.
(38) Ratner, D. M.; Adams, E. W.; Disney, M. D.; Seeberger, P. H. *ChemBioChem* **2004**, *5*, 1375–83.
(39) Hergenrother, P. J.; Depew, K. M.; Schreiber, S. L. *J. Am. Chem. Soc.* **2000**, *122*, 7849–50.
(40) MacBeath, G.; Koehler, A. N.; Schreiber, S. L. *J. Am. Chem. Soc.* **1999**, *121*, 7967–8.
(41) Barnes-Seeman, D.; Park, S. B.; Koehler, A. N.; Schreiber, S. L. *Angew. Chem., Int. Ed.* **2003**, *42*, 2376–9.
(42) Koehler, A. N.; Shamji, A. F.; Schreiber, S. L.; Barnes-Seeman, D.; Park, S. B. *J. Am. Chem. Soc.* **2003**, *125*, 8420–1.
(43) Fukui, S.; Feizi, T.; Galustian, C.; Lawson, A. M.; Chai, W. *Nat. Biotechnol.* **2002**, *20*, 1011–7.
(44) Blixt, O.; et al. *Proc. Natl. Acad. Sci. U.S.A.* **2004**, *101*, 17033–8.
(45) Lee, M. R.; Shin, I. *Org. Lett.* **2005**, *7*, 4269–72.
(46) Details of chemical synthesis are provided in Supporting Information.
(47) Afanassiev, V.; Hanemann, V.; Wolfl, S. *Nucleic Acids Res.* **2000**, *28*, E66.
(48) Chan, T. R.; Hilgraf, R.; Sharpless, K. B.; Fokin, V. V. *Org. Lett.* **2004**, *6*, 2853–5.

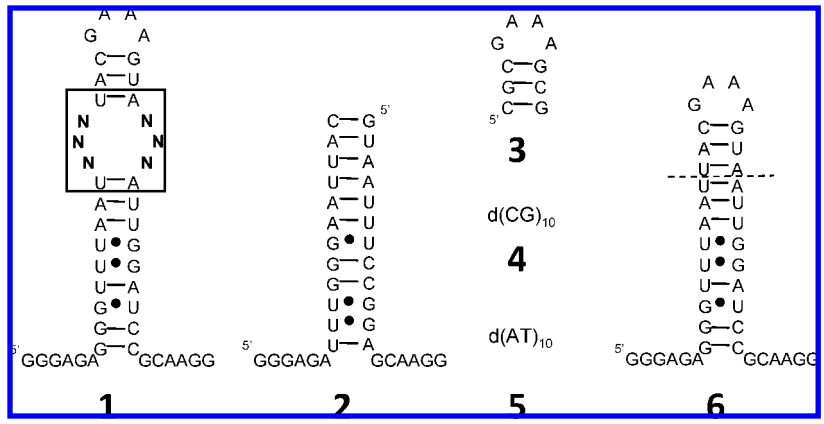

Figure 1. Secondary structures of the internal loop library (**1**, 4096 members) and competitor oligonucleotides **2**−**5**.[35,36] The competitor oligonucleotides were chosen to ensure RNA−ligand interactions occur with the random region in **1** and are RNA-specific. **6** is the empty cassette into which the random region was inserted. It serves as a control in fluorescence-based binding assays. The dashed line in **6** indicates where the random region was inserted to create **1**.

General Nucleic Acids. All DNA oligonucleotides were purchased from Integrated DNA Technologies Inc. (IDT, Coralville, IA) and used without purification unless noted otherwise. The RNA competitor oligonucleotides were purchased from Dharmacon (Lafayette, CO) and deprotected according to the manufacturer's standard procedure. All aqueous solutions were made with nanopure water.

RNA Library and Competitor Oligonucleotides. The RNA library (**1**) was designed to display a 3 × 3 nucleotide internal loop pattern[35,36] and was embedded in a hairpin cassette (**6**, Figure 1).[49] Library **1** was synthesized by in vitro transcription from the corresponding DNA template, which was custom-mixed at the randomized positions to ensure equivalent representation of all four nucleotides after deprotection. Competitor oligonucleotides were used to ensure that RNA−ligand interactions were confined to the random region. The two oligonucleotides that form **2** mimic the stem; the sequence was changed so that it does not bind to reverse transcription−polymerase chain reaction (RT-PCR) primers but maintains the nearest neighbors (Figure 1). Competitor **3** is a mimic of the hairpin loop displayed in **1**, while DNA oligonucleotides **4** and **5** ensure that interactions are RNA-specific.

RNA Transcription and Purification. RNA oligonucleotides were transcribed by use of an RNAMaxx transcription kit (Stratagene) with 5 μL of the amplified DNA from the PCR reaction described below or 1 pmol of DNA template purchased from IDT according to the manufacturer's protocol. After transcription, 0.5 unit of RQ DNase I (Promega) was added, and the sample was incubated for an additional 30 min at 37 °C.

The transcribed RNAs were then purified by gel electrophoresis on a denaturing 15% or 17% polyacrylamide gel. The RNAs were visualized by UV shadowing and extracted into 300 mM NaCl by tumbling overnight at 4 °C. The resulting solution was concentrated with 2-butanol and ethanol-precipitated. The pellet was resuspended in 200 μL of diethyl pyrocarbonate- (DEPC-) treated water, and the concentrations were determined by their absorbances at 260 nm and the corresponding extinction coefficients. Extinction coefficients were determined by use of HyTher version 1.0 (Nicolas Peyret and John SantaLucia, Jr., Wayne State University).[50,51] These parameters were calculated from information on the extinction coefficients of nearest neighbors in RNA.[52]

Internally labeled internal loop library was synthesized by including half the amount of cold ATP per the manufacturer's protocol and 4 μL of [α-^{32}P]ATP (3000 Ci/mmol; PerkinElmer, Waltham, MA) in the transcription reaction.

RNA Selection. Internally labeled internal loop library (**1**, 12 pmol) and competitor oligonucleotides (**2**−**5**, 20 nmol each) (Figure 1) were annealed separately in 1× hybridization buffer [HB1; 20 mM *N*-(2-hydroxyethyl)piperazine-*N*′-2-ethanesulfonic acid (Hepes), pH 7.5, 140 mM NaCl, and 5 mM KCl] at 60 °C for 5 min and allowed to slow-cool on the benchtop. $MgCl_2$ was then added to a final concentration of 1 mM. The annealed RNAs were mixed together for a total volume of 400 μL. Azido-aminoglycoside microarrays were pre-equilibrated with 1× hybridization buffer supplemented with 1 mM $MgCl_2$ and 40 μg/mL bovine serum albumin (BSA) (HB2) for 5 min at room temperature to prevent nonspecific binding. After the slides were pre-equilibrated, the annealed RNAs were pipetted onto the slide and evenly distributed across the slide surface with a custom-cut piece of Parafilm. The slides were hybridized at room temperature for 30 min, at which point the RNA solution was removed. The slides were washed by submersion in 30 mL of HB2 for 30 min with gentle agitation. This step was repeated. Excess buffer was removed from the slides, and the slides were dried.

The arrays were exposed to a phosphorimager screen and imaged using a Bio-Rad FX phosphorimager. The image was used as a template to mechanically remove selected RNAs from the surface. A 200 nL aliquot of HB1 was added to the spot to be removed. After 30 s, excess buffer (the majority of buffer was reabsorbed by the surface) was pipetted from the surface and the gel at that position on the surface was excised.

Reverse Transcription−Polymerase Chain Reaction Amplification. The agarose containing bound RNAs that was removed from the slide surface was placed into a thin-walled PCR tube with 18 μL of H_2O, 2 μL of 10× RQ DNase I buffer, and 2 units of RQ DNase I (Promega, Madison, WI). The tube was vortexed and centrifuged for 4 min at 8000*g*. The tube was then incubated at 37 °C for 2 h. The reaction was quenched by addition of 2 μL of 10× DNase stop solution (Promega, Madison, WI), and the sample was incubated at 65 °C for 10 min to completely inactivate the DNase. Aliquots of this solution were used for RT-PCR amplification. Reverse transcription reactions were completed in 1× RT buffer (supplied by the manufacturer), 1 mM dNTPs, 5 μM RT primer (5′-CCTTGCGGATCCAAT), 200 μg/mL BSA, 3.5 units of reverse transcriptase (Life Sciences, Inc., St. Petersburg, FL), and 20 μL of the selected RNAs treated with DNase I and incubated at 60 °C for 1 h. To 20 μL of the RT reaction were added 6 μL of 10× PCR buffer (1× PCR buffer is 10 mM Tris, pH 9, 50 mM KCl, and 0.1% Triton X-100), 4 μL of 100 μM PCR primer (5′-GGCCGGATCCTAATACGACTCACTATAGG-GAGAGGGTTTAAT), 2 μL of 100 μM RT primer, 0.6 μL of 250

(49) Bevilacqua, J. M.; Bevilacqua, P. C. *Biochemistry* **1998**, *37*, 15877–84.
(50) Peyret, N.; Seneviratne, P. A.; Allawi, H. T.; SantaLucia, J., Jr *Biochemistry* **1999**, *38*, 3468–77.
(51) SantaLucia, J., Jr *Proc. Natl. Acad. Sci. U.S.A.* **1998**, *95*, 1460–5.
(52) Puglisi, J. D.; Tinoco, I., Jr *Methods Enzymol.* **1989**, *180*, 304–25.

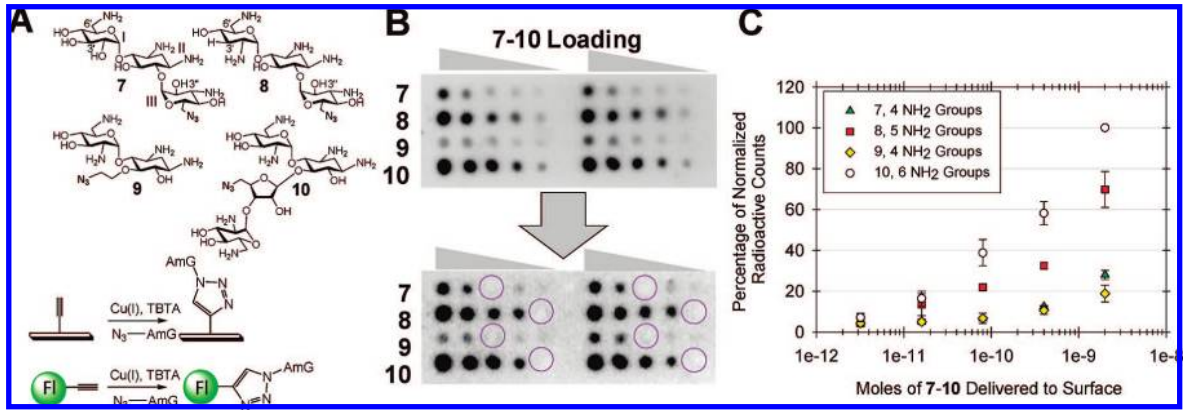

Figure 2. (A, top), Chemical structures of the azido-aminoglycosides used in this study: **7** (kanamycin A derivative), **8** (tobramycin derivative), **9** (neamine derivative), and **10** (neomycin B derivative). (A, bottom) Immobilization of **7**−**10**[35,37] onto alkyne-displaying agarose microarrays for 2DCS or conjugation to fluorescein (green ball) via a Huisgen dipolar cycloaddition reaction to study binding affinities; AmG refers to aminoglycoside. (B) Image of a microarray composed of **7**−**10** after hybridization with the oligonucleotides shown in Figure 1 (top) and after removal of bound RNA (bottom). Circles indicate positions where RNA was harvested. (C) Plot of data for binding of ^{32}P-internally labeled **1** by array-immobilized **7**−**10** in the presence of competitor oligonucleotides **2**−**5**. The signals in the plot were normalized relative to the highest signal obtained for binding **10**.[35] Panel B has been modified from ref 35.

mM $MgCl_2$, and 0.1 μL of Taq DNA polymerase. PCR cycling conditions (2-steps) were 95 °C for 1 min and 72 °C for 1 min.[49] Aliquots of the RT-PCR were checked every five cycles starting at cycle 10 on a denaturing 17% polyacrylamide gel stained with ethidium bromide or SYBR Gold (Invitrogen, Carlsbad, CA).

Cloning and Sequencing. The RT-PCR products were cloned into pGEM T Vector (Promega, Madison, WI) according to the manufacturer's protocol with 2 μL of the RT-PCR product. The ligation mixture was incubated overnight at room temperature, and then a 5 μL aliquot was transformed into DH5-α *Escherichia coli*. White colonies were used to inoculate 1 mL of TB medium containing 50 mg/L ampicillin in a well of a square, deep-well 96-well plate. The plate was shaken for 24−48 h at 37 °C until the cultures reached $OD_{600} > 4$. The cultures were pelleted and sent to Functional Biosciences Inc. (Madison, WI) for sequencing.

PCR Amplification of DNA Templates Encoding Selected RNAs. The DNA templates encoding the selected RNAs were PCR-amplified from the harvested plasmid DNA (Eppendorf Fast Plasmid Mini kit) in 50 μL of 1× PCR buffer, 4.25 mM $MgCl_2$, 0.33 mM dNTPs, 2 μM each primer (RT and PCR primers), and 0.1 μL of Taq DNA polymerase. The DNA was amplified by 25 cycles of 95 °C for 30 s, 50 °C for 30 s, and 72 °C for 1 min. All PCR reactions were checked by gel electrophoresis on a 5% agarose gel stained with ethidium bromide.

RNA Secondary Structure Prediction and Identification of Trends in Selected RNAs. The secondary structures of all selected RNAs were predicted by free energy minimization using the *RNAstructure* program.[53,54] The structures were then inspected for commonalities. To determine if the commonalities and trends were statistically significant, the percentage of RNAs displaying the trend in the selected RNAs was compared to the percentage of the RNAs that display that trend in the entire library. A *Z*-test was applied and the corresponding *p*-value was calculated. Please see Supporting Information for all calculations.

Fluorescence Binding Assays. Dissociation constants were determined by an in-solution, fluorescence-based assay. A selected RNA or RNA mixture was annealed in HB1 and 40 μg/mL BSA at 60 °C for 5 min and was allowed to slow-cool to room temperature. Then $MgCl_2$ and fluorescently labeled aminoglycoside (**7-Fl**, **8-Fl**, **9-Fl**, or **10-Fl**, Figure 2A) were added to final concentrations of 1 mM and 10 nM, respectively. Serial dilutions (1:2) were then completed in 1× HB2 + 10 nM fluorescently labeled azido-aminoglycoside. The solutions were incubated for 30 min at room temperature and then transferred to a well of a black 96-well plate. Fluorescence intensity was measured on a Bio-Tek FLX-800 plate reader. The change in fluorescence intensity as a function of RNA concentration was fit to[55]

$$I = I_0 + 0.5\Delta\varepsilon([FL]_0 + [RNA]_0 + K_t) - \{([FL]_0 + [RNA] + K_t)^2 - 4[FL]_0[RNA]_0)^{0.5}\}$$

where I is the observed fluorescence intensity, I_0 is the fluorescence intensity in the absence of RNA, $\Delta\varepsilon$ is the difference between the fluorescence intensity in the absence of RNA and in the presence of infinite RNA concentration, $[FL]_0$ is the concentration of the fluorescently labeled azido-aminoglycoside, $[RNA]_0$ is the concentration of the selected internal loop or control RNA, and K_t is the dissociation constant. Control experiments were also completed in the same manner for FITC-triazole,[35] which contains the dye and triazole linkage but no aminoglycoside.[56] No change in fluorescence is observed up to 5 μM **1** (entire internal loop library) or 3 μM Neo IL15, which was tested as a representative individual of the selected loops (Figures 1 and 5, respectively). These results show that the change in fluorescence is due to binding of the aminoglycoside to the oligonucleotides and not the dye itself.

Results and Discussion

Our library of azido-aminoglycosides was chosen for these studies because their parent aminoglycosides have been shown to bind bacterial rRNA A-sites.[57–63] The azido-aminoglycoside library (**7**−**10**, Figure 2A) was site-specifically immobilized onto alkyne-functionalized agarose arrays via a Huisgen 1,3 dipolar cycloaddition reaction to create chemical microarrays (Figure

(53) Mathews, D. H.; Disney, M. D.; Childs, J. L.; Schroeder, S. J.; Zuker, M.; Turner, D. H. *Proc. Natl. Acad. Sci. U.S.A.* **2004**, *101*, 7287–92.
(54) Mathews, D. H.; Sabina, J.; Zuker, M.; Turner, D. H. *J. Mol. Biol.* **1999**, *288*, 911–40.
(55) Wang, Y.; Rando, R. R. *Chem. Biol.* **1995**, *2*, 281–90.
(56) For details see Supporting Information.
(57) Moazed, D.; Noller, H. F. *Nature* **1987**, *327*, 389–94.
(58) Fourmy, D.; Recht, M. I.; Blanchard, S. C.; Puglisi, J. D. *Science* **1996**, *274*, 1367–71.
(59) Recht, M. I.; Fourmy, D.; Blanchard, S. C.; Dahlquist, K. D.; Puglisi, J. D. *J. Mol. Biol.* **1996**, *262*, 421–36.
(60) Lynch, S. R.; Gonzalez, R. L.; Puglisi, J. D. *Structure (Cambridge, MA, U.S.)* **2003**, *11*, 43–53.
(61) Wong, C. H.; Hendrix, M.; Priestley, E. S.; Greenberg, W. A. *Chem. Biol.* **1998**, *5*, 397–406.
(62) Ryu, D. H.; Rando, R. R. *Bioorg. Med. Chem.* **2001**, *9*, 2601–8.
(63) Griffey, R. H.; Hofstadler, S. A.; Sannes-Lowery, K. A.; Ecker, D. J.; Crooke, S. T. *Proc. Natl. Acad. Sci. U.S.A.* **1999**, *96*, 10129–33.

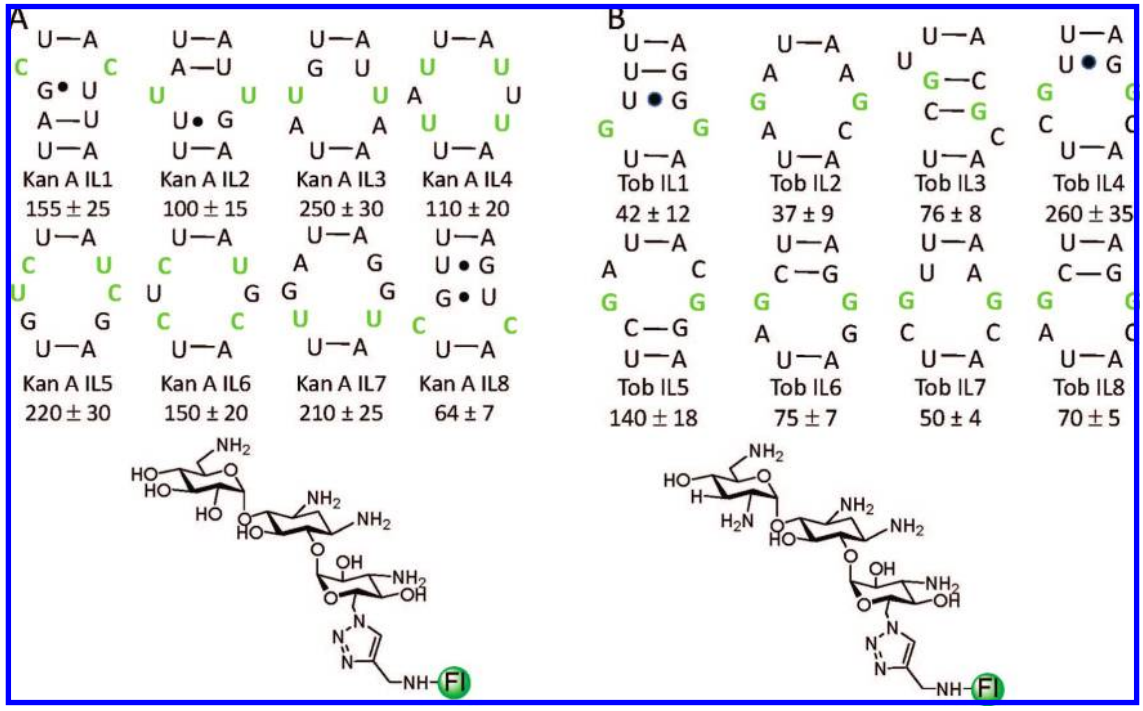

Figure 3. Secondary structures of the RNA internal loops that were selected to bind **7** (A, kanamycin A derivative) and **8** (B, tobramycin derivative) and their corresponding dissociation constants (nanomolar) (Figure 1). The nucleotides shown are derived from the boxed region in **1**. Analysis of these data shows that **7** prefers internal loops that contain potential pyrimidine−pyrimidine pairs (in green) and that **8** prefers internal loops that contain potential guanine−guanine pairs (in green). Tob IL3 may have a structure in equilibrium in which there is a 3 × 3 internal loop instead of the two bulges. Secondary structure studies with *RNAstructure*[53] predict that the 3 × 3 nucleotide loop is 3.2 kcal/mol less stable than the structure containing two 1-nucleotide bulges.

2A).[35–37,48,64] The position where the azido group was installed in each library member was governed by the ease of functionalizing a primary hydroxyl group.[35,37,65,66] In addition, crystal structures of kanamycin A (**7**-like) and tobramycin (**8**-like) complexed with an oligonucleotide mimic of the bacterial rRNA A-site show that no contacts are formed between the A-site and either aminoglycoside's 6′-OH group.[67,68] Therefore, **7** and **8** would be immobilized in a manner that mimics their biological presentations, at least for their binding to the bacterial rRNA A-site. Structures **9** (neamine-like) and **10** (neomycin B-like) were functionalized at the chosen positions (5- and 5″-OH, respectively) because both present rings I and II in similar manners, potentially allowing for RNA motifs that interact with these rings to be identified via analysis of the selection data from the two compounds. In contrast to the sites of functionalization with **7** and **8**, interactions are observed between the 5- and the 5″-OH groups in neamine and neomycin B, respectively, and an oligonucleotide mimic of the bacterial rRNA A-site.[67]

Aminoglycoside arrays were probed for binding to a ^{32}P-internally labeled RNA library that displays a 3 × 3 nucleotide internal loop pattern (**1**, Figures 1 and 2B).[35,36] The random region was embedded in oligonucleotide **6**, and the RNA motifs displayed by **1** include 1080 1 × 1 internal loops, 1200 2 × 2 internal loops, 1600 3 × 3 internal loops (some 3 × 3 internal loops can form two 1-nucleotide bulges; see Tob IL3 in Figure 3), and 216 unique base-paired regions. One potential problem with using **1** to identify RNA loop−ligand interactions is that interactions can occur outside of the random region. This would cause selection of all library members. To deal with this issue, competitor oligonucleotides (Figure 1) were used that mimic the stem (**2**) and the hairpin (**3**) in **1** to compete off these interactions. DNA oligonucleotides **4** and **5** were also added as competitors to ensure that RNA-specific interactions were selected. Array hybridization (Figure 2B) was completed with 20 nmol of each competitor oligonucleotide and 12 pmol of **1**; the large excess of competitors was used to ensure that it is in excess of both the loading of **7**−**10** onto the surface and **1**.

Hybridization of the arrays under the conditions above showed a clear dose response and the aminoglycosides bound different amounts of **1** (Figure 2B,C). Plots of the normalized signal for binding of **1** showed, not surprisingly, that the signal scaled with the number of amino groups present on the aminoglycosides (Figure 2C). Bound RNAs were harvested from the arrays via excision of the agarose at the positions indicated in Figure 2B. Excision of the bound RNAs is possible because of the unique features of the agarose microarray: ligands can be site-specifically immobilized onto the surface for screening, and rehydration of the surface allows for the positions where RNA is bound to ligand to be harvested via simple gel extraction.[35] These bound RNAs can be amplified by RT-PCR, cloned, and sequenced to identify the binders. The lowest signal (or ligand loading) spots that were able to be amplified over background were harvested because RNAs that bind at lower ligand loading are higher affinity.[35] The mixtures of selected RNA motifs were then amplified via RT-PCR, transcribed into RNA, and studied for binding each aminoglycoside via a

(64) Kolb, H. C.; Finn, M. G.; Sharpless, K. B. *Angew. Chem., Int. Ed.* **2001**, *40*, 2004–2021.
(65) Michael, K.; Wang, H.; Tor, Y. *Bioorg. Med. Chem.* **1999**, *7*, 1361–71.
(66) Wang, H.; Tor, Y. *Angew. Chem., Int. Ed.* **1998**, *37*, 109–11.
(67) Francois, B.; Russell, R. J.; Murray, J. B.; Aboul-ela, F.; Masquida, B.; Vicens, Q.; Westhof, E. *Nucleic Acids Res.* **2005**, *33*, 5677–90.
(68) Vicens, Q.; Westhof, E. *Chem. Biol.* **2002**, *9*, 747–55.

Table 1. Binding of **1**, **6**, and Libraries of Selected RNAs to Different Aminoglycosides[a]

	aminoglycoside from which bound RNAs were harvested[b]				other RNAs		
aminoglycoside	**7**	**8**	**9**	**10**	**1**	**6**	A-site[c]
7	75 ± 15; −	>1500; >30	>1500; >7	1100 ± 113; 6	>1200	>5000	18000
8	850 ± 105; 11	50 ± 12; −	>1000; >11	800 ± 95; 5	>1200	~2500	1500
9	900 ± 03; 12	>1500; >30	200 ± 33; −	1100 ± 127; 6	>2500	>5000	7800
10	625 ± 82; 8	700 ± 84; 14	500 ± 53; 2.5	160 ± 20; −	1200 ± 112	1600 ± 212	19

[a] All dissociation constants are reported in nanomolar. Selectivies (given after the semicolon) were calculated by dividing the K_d for the other aminoglycoside by the K_d for the aminoglycoside that the loop was selected to bind. [b] These are the pools of RNA structures that were selected to bind each aminoglycoside. [c] Binding affinities for an oligonucleotide mimic of the bacterial rRNA A-site were measured using surface plasmon resonance (SPR) with the RNA immobilized onto the SPR chip.[61]

fluorescence-based emission assay with fluorescein-labeled **7**−**10**, denoted **7-Fl**, **8-Fl**, **9-Fl**, and **10-Fl** (Figure 2A).[35]

Specificity in the RNA Motif−Aminoglycoside Partners Identified by 2DCS. Table 1 summarizes the dissociation constants determined for all selected RNA mixtures, the entire RNA library (**1**, Figure 1), and the empty hairpin cassette (**6**, Figure 1) for all aminoglycoside derivatives. The mixtures of selected RNAs bind to their respective ligand with K_d values from 75 to 200 nM. In comparison, binding to the whole library, **1**, was ≥1200 nM and binding to the empty cassette, **6**, was ≥1600 nM for all aminoglycosides. These experiments were completed at pH 7.5 in a buffer containing 1 mM $MgCl_2$, while those completed in our previous report were completed at pH 7.0 without $MgCl_2$.[35] Higher pH, the presence of divalent metal ions, and an increase in ionic strength all decrease aminoglycoside binding affinity and help explain the differences in the dissociation constants between the two studies.[35,69–71] The new conditions were used because they more closely mimic physiological conditions than the previous buffer. Not surprisingly, the neomycin B mimetic (**10**) with the largest number of amines, exhibits the highest affinities toward **1** and **6**, suggesting it has a significant nonspecific binding mode. This has also been observed in studies of aminoglycosides binding to mimics of the bacterial rRNA A-site.[61] Additionally, competition dialysis studies with a series of nucleic acids showed neomycin binds helical A-form nucleic acids that are present in the nonvariable region of **1**.[72]

The binding of the selected RNA mixtures to the other arrayed aminoglycosides was studied to determine whether the selected structures are specific for the aminoglycoside that they were selected to bind. Interestingly, the RNAs selected to bind **7** and **8** are >8-fold and ≥14-fold specific, respectively, for their corresponding aminoglycosides. Lower specificities are observed between structures selected to bind **9** (neamine-like) and **10** (neomycin B-like); in the worst case, there was only a 2.5-fold specificity between the RNAs selected to bind **9** for binding **10**. This is not surprising since they have rings I and II in common (Figure 2A), making it likely that these two structures bind overlapping RNA motif space.

Studies on the Specific RNA Motifs Selected To Bind 7−10. To deconvolute the specific RNA structures that were selected, the mixtures of RNAs selected to bind **7**−**10** were cloned and sequenced and their secondary structures were modeled with the *RNAstructure* program (Figures 3–5).[53,54] The data were then statistically analyzed and *p*-values were

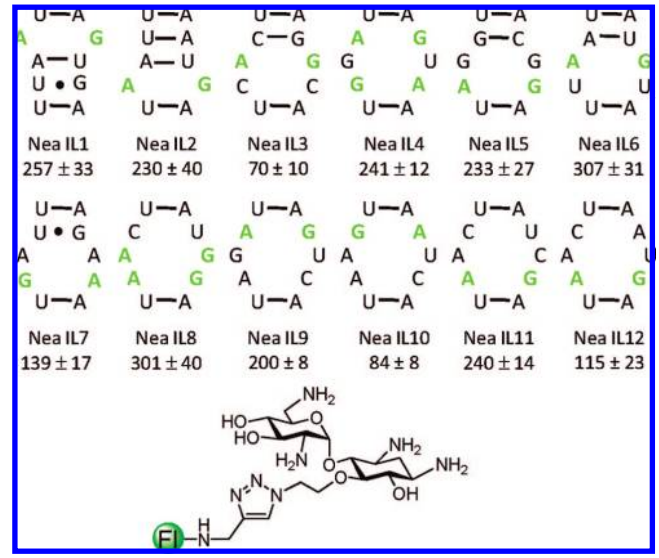

Figure 4. Secondary structures of the RNA internal loops that were selected to bind **9** (neamine derivative) and their corresponding dissociation constants (nanomolar). The nucleotides shown are derived from the boxed region in **1** (Figure 1). Analysis of these data shows preferences for internal loops that contain potential guanine−adenine pairs (in green).

computed for groups of the selected structures to find RNA structure trends in the data. Trends in RNA structure space were observed for aminoglycosides **7** (Figure 3A), **8** (Figure 3B), and **10** (Figure 5). Compound **7** prefers pyrimidine-rich internal loops (Figure 3A), in particular internal loops displaying potential UU pairs (two-tailed p-value = 0.0373), while **8** prefers internal loops that display potential GG pairs (Figure 3B, two-tailed p-value = 0.0109). Compound **10** prefers internal loops that display potential GA pairs (Figure 5, two-tailed p value = 0.0019), which is also the most highly represented type of internal loop for **9** (Figure 4). This could explain, at least in part, the smaller specificity between structures selected to bind **9** and **10** (Table 1). Further inspection of the GA-containing internal loops that bind **9** show that 66% of the other nucleotides in the internal loop (i.e., non-GA) that are un- or noncanonically paired are pyrimidines; this trend is not observed for the internal loops that bind **10**.

Dissociation constants were determined for each statistically significant RNA motif-ligand pair. Figures 3–5 show the secondary structures of selected internal loops and their dissociation constants. The ranges of dissociation constants are consistent with the dissociation constants for the RNA mixtures (Table 1).

In general 1 × 1, 2 × 2, and 3 × 3 internal loops are well represented for each of the ligands (Figures 3–5). Further analysis of the global structures shows that some general features

(69) Thomas, J. R.; Liu, X.; Hergenrother, P. J. *Biochemistry* **2006**, *45*, 10928–38.
(70) Tor, Y.; Hermann, T.; Westhof, E. *Chem. Biol.* **1998**, *5*, R277–83.
(71) Hermann, T.; Westhof, E. *J. Mol. Biol.* **1998**, *276*, 903–12.
(72) Arya, D. P.; Xue, L.; Willis, B. *J. Am. Chem. Soc.* **2003**, *125*, 10148–9.

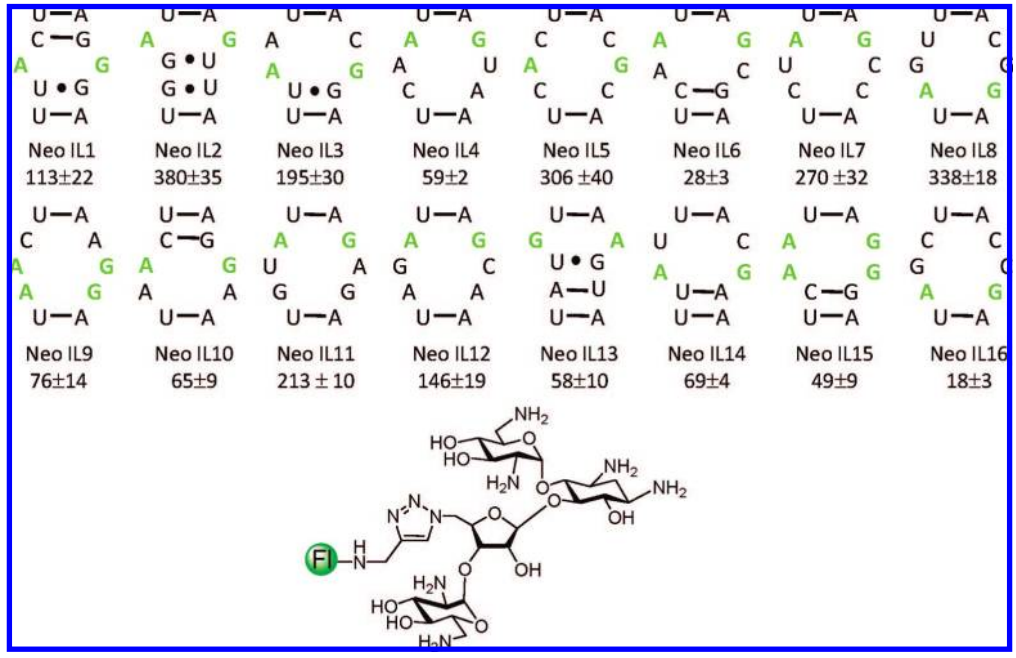

Figure 5. Secondary structures of the RNA internal loops that were selected to bind **10** (neomycin B derivative) and their corresponding dissociation constants (nanomolar). The nucleotides shown are derived from the boxed region in **1** (Figure 1). Analysis of these data shows preferences for internal loops that contain potential guanine−adenine pairs (in green).

can be found in the 1 × 1 internal loops (Figures 3–5). For all of the selected 1 × 1 internal loops, there is an underrepresentation of internal loops with GC closing pairs; of the eight 1 × 1 internal loops selected, only one loop has a single closing GC pair (Neo IL1, binds **10**) and none are closed with two GC pairs. In addition, all of the internal loops but one (Nea IL2, binds **9**) have at least one GU closing pair. Similar results have been found with internal loops selected to bind 6′-*N*-5-hexynoate kanamycin A.[35] These collective results suggest the thermodynamic stability of the 1 × 1 loops is an important determinant in molecular recognition because there is a 1.2 kcal/mol penalty for closing a loop with an AU or GU pair instead of a GC pair.[73] Perhaps in the presence of ligand these pairs partially form or do not form at all. This may indicate an induced-fit type of binding; conformational changes in RNA often occur upon binding to ligand.[74–77] Structural studies must be completed to test this hypothesis, however.

Comparison of the groups of RNA motifs selected to bind each aminoglycoside show that there are similar features in each group that go beyond the presence of a potential loop noncanonical pair. Many loops share common closing pairs or share some other loop feature. For example, with compound **7** (Figure 3A), Kan A IL1 and Kan A IL8 each have a 1 × 1 CC internal loop closed by a GU and an AU pair but are different in their orientations. Loop Kan A IL2 appeared twice in the sequencing data and is also an all-pyrimidine (UU) 1 × 1 internal loop that is also closed by a GU and an AU pair. For compound **8** (Figure 3B), five of the eight loops that have potential GG pairs were 2 × 2 internal loops (Tob IL4−8). Both Tob IL4 and Tob IL7 have a 5′-CG-3′/3′-CG-5′ internal loop but with different closing pairs. The Tob IL5 and Tob IL8 internal loops are similar, 5′-GA-3′/3′-GC-5′ and 5′-AG-3′/3′-CG-5′, respectively, and both are closed with GC and AU pairs that are oriented in the same manner relative to the loop nucleotides. For compound **9**, two 1 × 1 GA internal loops (Nea IL1 and Nea IL2) were identified that are closed by AU pairs in different orientations. The four 2 × 2 internal loops (Nea IL3, IL5, IL6, and IL7) each have either a pyrimidine across from a pyrimidine (Nea IL3 and IL6) or a purine across from a purine (Nea IL5 and IL7) adjacent to the potential GA pair. Four of the 3 × 3 internal loops identified for binding **9** have an adenine across from cytosine in the internal loop (Nea IL9−12). Of these four, three (Nea IL9, Nea IL10, and Nea IL12) have the adenine across from the cytosine in a position that is adjacent to the internal loop-closing AU pair, and there are also nucleotides that can form pairs (GU or AU) in the internal loop's central position (Figure 4). These results may indicate the central position is paired (GU or AU) in these internal loops. For loops that bind **10** (Figure 5), each of the 1 × 1 GA internal loops has at least one closing GU pair (Neo IL1, Neo IL2, and Neo IL13). For the 2 × 2 internal loops, Neo IL3 and IL6 have the same loop composition with an adenine across from a cytosine in addition to an adenine across from a guanine, but the orientation of the internal loop and the loop closing pairs are different. For the eight 3 × 3 internal loops selected to bind **10**, four have nucleotides that can form canonical pairs in the loop's central position (Neo IL4, Neo IL11, Neo IL12, and Neo IL16), which is similar to observations with **9**.

Once the specific RNA motifs interacting with ligands were identified, studies on the specificity of a selected RNA for the corresponding aminoglycoside were revisited. Dissociation constants were measured for 16 selected RNAs for binding to each of **7**−**10-Fl** (Table 2). Specificities range from 2- to 80-fold depending on the aminoglycoside and the internal loop studied. The average specificity for these subsets of internal

(73) Davis, A. R.; Znosko, B. M. *Biochemistry* **2007**, *46*, 13425–36.
(74) Hermann, T.; Patel, D. J. *Science* **2000**, *287*, 820–5.
(75) Gosser, Y.; Hermann, T.; Majumdar, A.; Hu, W.; Frederick, R.; Jiang, F.; Xu, W.; Patel, D. J. *Nat. Struct. Biol.* **2001**, *8*, 146–50.
(76) Puglisi, J. D.; Tan, R.; Calnan, B. J.; Frankel, A. D.; Williamson, J. R. *Science* **1992**, *257*, 76–80.
(77) Fourmy, D.; Yoshizawa, S.; Puglisi, J. D. *J. Mol. Biol.* **1998**, *277*, 333–45.

Table 2. Binding and Selectivities of Single Internal Loops Selected from **7**−**10**

	dissociation constants (nM); selectivity for binding **7**−**10-Fl**[a]			
internal loop	**7-Fl**	**8-Fl**	**9-Fl**	**10-Fl**
	Selected from **7**			
Kan A IL2	100 ± 15	778 ± 60; 7	>1200[b]; 12[c]	>1500[b]; 12[c]
Kan A IL4	110 ± 20	780 ± 48; 7	>2000[d]; 18[c]	1100 ± 192; 10
Kan A IL6	150 ± 20	300 ± 26; 2	>2250[d]; 15[c]	580 ± 50; 4
Kan A IL8	64 ± 7	>2250[b]; 35[c]	>2250[d]; 35[c]	685 ± 84; 11
	Selected from **8**			
Tob IL1	>1200[b]; 29[c]	42 ± 12	655 ± 18; 16	342 ± 20; 8
Tob IL2	690 ± 22; 19	37 ± 9	>2250[d]; 61[c]	1600 ± 28; 43
Tob IL7	1400 ± 280; 28	50 ± 4	>2250[d]; 45[c]	930 ± 42; 19
Tob IL8	560 ± 62; 8	70 ± 5	>2250[d]; 32[c]	660 ± 63; 9
	Selected from **9**			
Nea IL2	490 ± 15; 2	960 ± 70; 4	230 ± 40	850 ± 77; 2
Nea IL3	780 ± 58; 11	840 ± 28; 12	70 ± 10	542 ± 35; 8
Nea IL6	>2250[d]; 7[c]	640 ± 20; 2	307 ± 31	1435 ± 15; 5
Nea IL10	860 ± 4; 10	1050 ± 120; 13	84 ± 8	1000 ± 144; 12
	Selected from **10**			
Neo IL6	620 ± 75; 22	>2250[d]; 80[c]	>2250[d]; 80[c]	28 ± 3
Neo IL9	>2250[d]; 30[c]	860 ± 50; 11	580 ± 4; 8	76 ± 14
Neo IL13	460 ± 47; 8	920 ± 85; 16	>2250[d]; 39[c]	58 ± 10
Neo IL15	1150 ± 130; 23	>2250[d]; 46[c]	>2250[d]; 46[c]	49 ± 9

[a] Selectivities (given after the semicolon) were calculated by dividing the K_d for the other aminoglycoside by the K_d for the aminoglycoside that the loop was selected to bind. [b] These values are a lower limit of the dissociation constants because the titration curves did not reach saturation at these concentrations. [c] These values represent a lower limit of specificity. [d] In these binding experiments there was no change in fluorescence observed.

loops is 14-, 26-, 7-, and 34-fold for **7**, **8**, **9**, and **10**, respectively. The highest specificity was measured for Neo IL6 that was selected for binding to **10**, which binds 22-, 80-, and 80-fold more weakly to **7-Fl**, **8-Fl**, and **9-Fl**, respectively. Other high specificity RNA motif−ligand pairs are **7** and Kan A IL8 with an average specificity of 27-fold, **8** and Tob IL2 with an average specificity of 41-fold, and **9** and Nea IL10 with an average specificity of 12-fold. The lower specificity for **9** is also mirrored in the specificity results observed for binding to the entire mixture of selected structures (Table 1). Interestingly, the 1 × 1 GA internal loop selected to bind **9** (Nea IL2) has the lowest selectivity for binding the different aminoglycosides (average specificity of 2.6-fold) of all internal loops tested for specificity. This loop and Nea IL1 are both closed with AU pairs. In contrast, the single GA internal loops (Neo IL1, Neo IL2, and Neo IL13) selected to bind **10** have at least one loop closing GU pair. One of these loops (Neo IL13) was tested for aminoglycoside specificity and binds 39-fold more weakly to **9-Fl** than **10-Fl**. Evidently, the identity of the loop closing pairs can affect aminoglycoside selectivity with 1 × 1 internal loops.

A particular challenge in finding ligands that bind RNA has been to identify specific aminoglycoside−RNA partners. The observation that mixtures of selected RNA structures and individual selected RNAs exhibit specificities for the different aminoglycosides is encouraging in this regard. This is especially true given the fact that RNAs selected for **7** and **8** bind at least 8-fold more tightly to their respective ligands than to **10**, which has more NH_2 groups and binds to the bacterial rRNA A-site 950- and 78-fold more tightly than **7** and **8**, respectively (Table 1).[61] These results suggest that specific interactions between the aminoglycosides and RNA motifs identified in these selections are dependent on the aminoglycoside size and shape and the features in the RNA, not simply charge−charge interactions.

One question that arises is "Why does 2DCS allow for the selection of specific aminoglycoside−RNA internal loop interactions?" A likely possibility is the nature of microarray-based screening that sets up a competition experiment on the surface of an array between the four arrayed ligands and members of **1**. Such a competition is possible because **1** is being exposed to each of the four aminoglycosides simultaneously during hybridization and the amount of aminoglycoside delivered to an array is in excess (4.6 nmol)[37,78] over the amount of **1** hybridized (12 pmol), 380-fold excess total aminoglycoside over **1**.

Results for Inserting Internal Loops into Other Cassettes: Are Cassette Nucleotides Important for Binding? To determine if specific RNA internal loop−ligand partners were selected, we changed the cassette in which the internal loops were displayed (**11**, Figure 6) by changing the AU and GU pairs in **6** to GC pairs. This was done because previous experiments have shown that that 2-deoxystreptamine (2-DOS) binds weakly to GU pairs and GU steps in RNA,[79] which are present in **6** (Figure 1). The simplest statistically significant internal loops (1 × 1 nucleotide) and their nearest neighbors were inserted into **11**. The nearest neighbors were included because previous experiments have shown that internal loop nearest neighbors can affect internal loop structure[80,81] and because of the thermodynamic arguments for loop closing pairs raised above. Results show that dissociation constants for the four internal loops tested are similar when they are displayed in either **6** or **11** (Figure 6). As also demonstrated for a selection to identify RNA internal loop preferences for a 6′-N-derivatized kanamycin A,[35] these results show that cassette nucleotides do not contribute significantly to aminoglycoside affinity and that the selected RNA motif−ligand pairs are portable.

Comparison to Other Studies on RNAs That Bind Aminoglycosides. We have probed chemical and RNA spaces simultaneously in order to determine the RNA sequence or structure that is preferred by four related aminoglycoside derivatives (Figure 7). The kanamycin A derivative, **7**, shows a preference for pyrimidines, in particular loops containing potential UU pairs. Interestingly, 6′-*N*-5-hexynoate kanamycin was previously found to prefer RNA internal loops that can form potential AC[35] and UU pairs.[36] This suggests that these two related structures (**7** and 6′-*N*-5-hexynoate kanamycin A) can bind to similar RNA motifs. The bacterial rRNA A-site also contains a UU pair, and a crystal structure of the bacterial rRNA A-site complexed with several aminoglycosides has been reported.[67] Direct contacts are made between kanamycin and the UU pair in the A-site, though this contact also occurs with tobramycin. Comparison of the contacts between kanamycin A and tobramycin and the bacterial rRNA A-site show that 21 and 20 contacts are formed, respectively.[67,68] Of these contacts, only eight are present in both complexes. This indicates that the two related aminoglycosides have somewhat different structures in their bound state with the A-site, suggesting that they may also bind different RNA space. Indeed we have found that tobramycin-like **8** binds

(78) Using a fluorescamine-based assay described in ref 37, it was determined for the highest concentration of aminoglycoside spotting solution that 48%, 62%, 79%, and 36% of the aminoglycoside delivered to the array surface is immobilized for **7**, **8**, **9**, and **10**, respectively.
(79) Yoshizawa, S.; Fourmy, D.; Eason, R. G.; Puglisi, J. D. *Biochemistry* **2002**, *41*, 6263–70.
(80) Wu, M.; Turner, D. H. *Biochemistry* **1996**, *35*, 9677–89.
(81) SantaLucia, J., Jr.; Turner, D. H. *Biochemistry* **1993**, *32*, 12612–23.

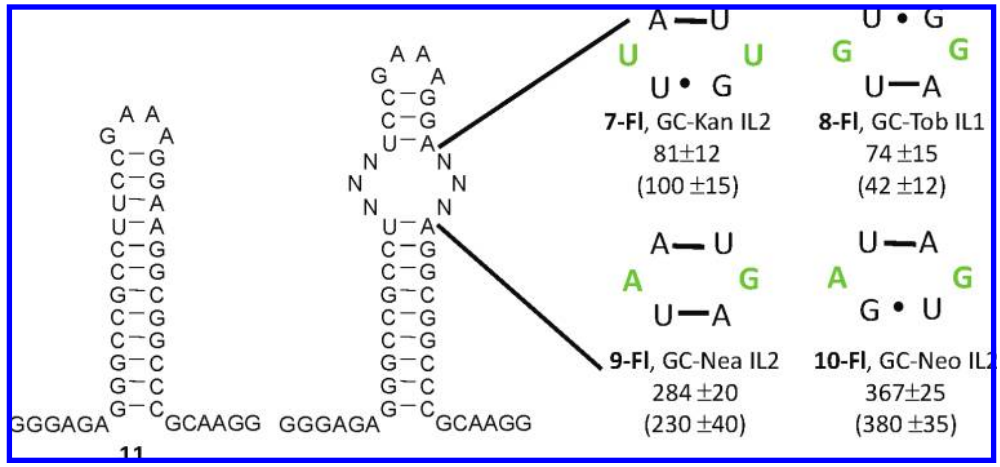

Figure 6. Secondary structures of the simplest loops selected to bind each aminoglycoside derivative and the alternative cassette (**11**) in which they were embedded. All GU and AU pairs were changed to GC pairs in **11** to determine whether cassette nucleotides contribute to binding affinity. Dissociation constants for the loops are below the secondary structures and are reported in nanomolar. Dissociation constants for the loops in the original cassette (**6**, Figure 1) are in parentheses. The GC cassette alone (**11**) binds weakly to **7**−**10-Fl** with dissociation constants ≥2 μM. *In each case the binding constants of the ligands are similar when the internal loops are displayed in the different cassettes, showing that interactions to cassette nucleotides are not important for binding.*

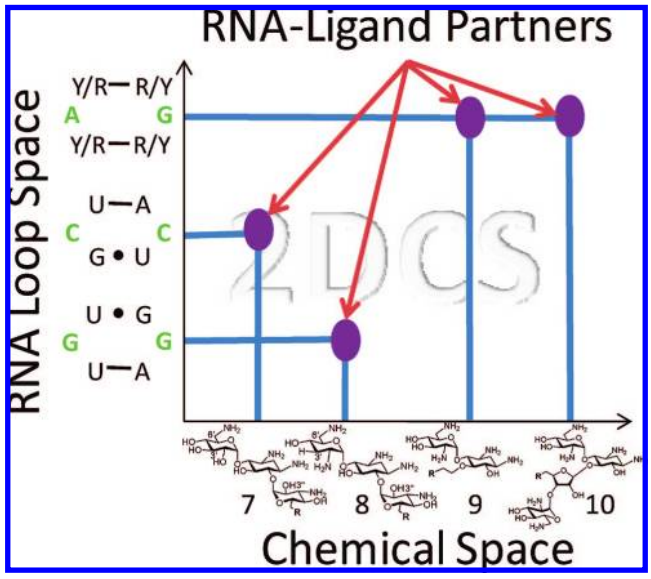

Figure 7. Schematic representation of the 2DCS data reported in this study. By probing both RNA and chemical spaces simultaneously, two aminoglycoside derivatives (tobramycin and kanamycin A) prefer to bind different RNA spaces while two other aminoglycoside derivatives (neamine and neomycin B) prefer to bind overlapping RNA space, presumably because they share the top two rings in their structures.

to different RNA structures than kanamycin A-like **7**, in support of this hypothesis.

One method to introduce or affect the specificity of aminoglycosides may therefore be to restrict the conformations they can sample or alter the conformation altogether. Indeed, several groups have synthesized and studied aminoglycosides that have been rigidified by introducing additional ring systems.[82–86] It would be interesting to see how constraining the three-dimensional space that these rigidified aminoglycosides can sample affects the RNA space the ligands recognize.

Aminoglycoside **8** prefers loops that display potential GG pairs. Solution structures of tobramycin aptamers show that tracts of purines are important for selective binding; a guanine forms a cap for the aminoglycoside.[87–89] It is difficult to make direct comparisons to the previously reported tobramycin aptamer since it was selected by immobilization through the 6′-amine. Our tobramycin derivative was selectively immobilized through the 6″-amine. In the NMR structure of the tobramycin aptamer, the 6″-amine is buried within the RNA[87] and it is therefore unlikely that **8** could bind in a similar fashion.

Compound **10** prefers loops with potential GA pairs. A previously reported neomycin aptamer also contains a GA pair, which sits on top of neomycin. [90] This aptamer was selected by random attachment to a resin via either the 6′- or 6″-amine. On the basis of the orientation of neomycin in the solution structure, the authors postulated that the NMR structure is representative of the RNAs that bind when neomycin is immobilized through the 6″-amine since it is not buried within the RNA, while the 6′-amine is.[90] Our **10** neomcyin derivative was selectively immobilized through ring III, which is also not buried within the aptamer.

Compound **9** prefers loops with potential GA pairs over other types of mismatches (40% of the structures contain potential GA pairs), though it is not statistically significant. Because neamine is smaller than most aminoglycosides and has the largest cationic charge density, it likely can accommodate many more RNA folds. We are currently employing multiple rounds of selection in order to better define the RNA motif preferences for neamine.

(82) Blount, K. F.; Zhao, F.; Hermann, T.; Tor, Y. *J. Am. Chem. Soc.* **2005**, *127*, 9818–29.
(83) Zhao, F.; Zhao, Q.; Blount, K. F.; Han, Q.; Tor, Y.; Hermann, T. *Angew. Chem., Int. Ed.* **2005**, *44*, 5329–34.
(84) Kling, D.; Hesek, D.; Shi, Q.; Mobashery, S. *J. Org. Chem.* **2007**, *72*, 5450–3.
(85) Asensio, J. L.; Hidalgo, A.; Bastida, A.; Torrado, M.; Corzana, F.; Chiara, J. L.; Garcia-Junceda, E.; Canada, J.; Jimenez-Barbero, J. *J. Am. Chem. Soc.* **2005**, *127*, 8278–9.
(86) Bastida, A.; Hidalgo, A.; Chiara, J. L.; Torrado, M.; Corzana, F.; Perez-Canadillas, J. M.; Groves, P.; Garcia-Junceda, E.; Gonzalez, C.; Jimenez-Barbero, J.; Asensio, J. L. *J. Am. Chem. Soc.* **2006**, *128*, 100–16.
(87) Jiang, L.; Patel, D. J. *Nat. Struct. Biol.* **1998**, *5*, 769–74.
(88) Cho, J.; Hamasaki, K.; Rando, R. R. *Biochemistry* **1998**, *37*, 4985–92.
(89) Wang, Y.; Killian, J.; Hamasaki, K.; Rando, R. R. *Biochemistry* **1996**, *35*, 12338–46.
(90) Jiang, L.; Majumdar, A.; Hu, W.; Jaishree, T. J.; Xu, W.; Patel, D. J. *Structure* **1999**, *7*, 817–27.

Interestingly, neamine derivatives[91] and neomycin[92,93] have been shown to inhibit interactions between the protein Rev and the RRE RNA in HIV. The binding site of Rev and neomycin B in RRE have been mapped and show that these ligands interact at a site that contains a 3 × 2 RNA internal loop that contains GA and GG pairs.[92,93] Although the aminoglycoside binding site in RRE is an asymmetric internal loop, the similarities between the symmetric internal loops that we selected are interesting.

It should be noted that, in contrast to SELEX, RNA sequence preferences for kanamycin, tobramycin, and neomycin derivatives were identified using only a single round of selection. This is likely due to reduced size of **1** (4096 members) versus typical SELEX libraries (10^{13} to 10^{15} members)[19] and the use of competitor oligonucleotides (**2**−**5**) to select against binding to common elements in **6** and **1**, which also introduced stringency into the selection. An additional factor may also be the competition that is occurring for RNA−ligand partners on the array surface that is mentioned above. This may allow 2DCS to be of general use for the selection of selective RNA−ligand interactions.

Implications. Our results developed a set of consensus RNA internal loops that prefer derivatives of four aminoglycosides (Figure 7). In terms of understanding general features in RNA motifs that bind ligands, it will be interesting to see how the data described here for a library of symmetric loops correlate with 2DCS of asymmetric RNA internal loops or hairpin loops. Bioinformatics tools are already available to find RNA motifs in genomic sequences (RNAMotif).[94] Therefore, coupling the data described herein with searching tools may elucidate new RNA targets for aminoglycosides.

It should also be noted that aminoglycoside antibiotics display less than favorable toxicity profiles.[95] One challenge that 2DCS has not been tested for is identifying RNA motif−ligand partners with more druglike ligands, especially ones that have an unknown RNA binding capacity. The ability to probe both RNA and chemical spaces simultaneously, however, may allow 2DCS to identify such partners. These interactions could go undetected if only a single or a few biologically important RNAs were probed for binding to a chemical library. Although the challenge of enabling the rational and modular design of small molecules targeting RNA by use of a database of RNA motif−ligand pairs is daunting given the diversity of RNA structures present in nature, we hope that 2DCS will accelerate these developments by serving as an enabling technology.

Acknowledgment. We thank Professor Yitzak Tor (University of California, San Diego) for helpful suggestions and Olivia Barrett for completing the fluorescamine assay to determine aminoglycoside loading on the microarrays. This work was funded by the University at Buffalo, The State University of New York, The New York State Center of Excellence in Bioinformatics and Life Sciences, A NYSTAR J. D. Watson Award (M.D.D.), The Camille and Henry Dreyfus Young Investigator Award (M.D.D.), a Cottrell Scholar Award from the Research Corporation (M.D.D.), and the Kapoor endowment fund.

Supporting Information Available: Details on the synthesis of the fluorescently labeled azido-aminoglycosides **7**−**10-Fl**, results from statistical analysis of the selected structures, and representative fluorescence binding assays. This material is available free of charge via the Internet at http://pubs.acs.org.

JA803234T

(91) Park, W. K. C.; Auer, M.; Jaksche, H.; Wong, C. H. *J. Am. Chem. Soc.* **1996**, *118*, 10150–5.
(92) Werstuck, G.; Zapp, M. L.; Green, M. R. *Chem. Biol.* **1996**, *3*, 129–37.
(93) Zapp, M. L.; Stern, S.; Green, M. R. *Cell* **1993**, *74*, 969–78.
(94) Macke, T. J.; Ecker, D. J.; Gutell, R. R.; Gautheret, D.; Case, D. A.; Sampath, R. *Nucleic Acids Res.* **2001**, *29*, 4724–35.
(95) Silva, J. G.; Carvalho, I. *Curr. Med. Chem.* **2007**, *14*, 1101–19.